Thermodynamics of Quantum Trajectories on a Quantum Computer

Marcel Cech,[1] Igor Lesanovsky,[1,2] and Federico Carollo[1]
[1]Institut für Theoretische Physik, Universität Tübingen, Auf der Morgenstelle 14, 72076 Tübingen, Germany
[2]School of Physics and Astronomy and Centre for the Mathematics and Theoretical Physics of Quantum Non-Equilibrium Systems, The University of Nottingham, Nottingham NG7 2RD, United Kingdom

(Received 24 January 2023; revised 5 June 2023; accepted 17 August 2023; published 22 September 2023)

Quantum computers have recently become available as noisy intermediate-scale quantum devices. Already these machines yield a useful environment for research on quantum systems and dynamics. Building on this opportunity, we investigate open-system dynamics that are simulated on a quantum computer by coupling a system of interest to an ancilla. After each interaction the ancilla is measured, and the sequence of measurements defines a quantum trajectory. Using a thermodynamic analogy, which identifies trajectories as microstates, we show how to bias the dynamics of the open system in order to enhance the probability of quantum trajectories with desired properties, e.g., particular measurement patterns or temporal correlations. We discuss how such a biased—generally non-Markovian—dynamics can be implemented on a unitary, gate-based quantum computer and show proof-of-principle results on the publicly accessible `ibmq_jakarta` machine. While our analysis is solely conducted on small systems, it highlights the challenges in controlling complex aspects of open-system dynamics on digital quantum computers.

DOI: 10.1103/PhysRevLett.131.120401

Introduction.—A widely pursued quest in contemporary physics research concerns the realization of a universal quantum computer. However, while fundamental issues—such as scalability and the necessity of error correction—have been identified [1–5], the availability of a fault-tolerant machine, which is able to implement arbitrary unitary circuits, may still be years away. Currently available quantum computation platforms belong to the class of noisy intermediate-scale devices [5–7]. Nevertheless, these machines constitute intriguing systems for conducting proof-of-principle studies, for testing the efficient implementation of quantum algorithms, and for making conceptual progress in the understanding of the utility of quantum computers [8–22].

In this Letter we focus on open-system dynamics implemented on a quantum computer via unitary gates [20,23–29]. The basis for this approach is the so-called collision model [20,30–33]. Here irreversible open-system dynamics is generated by creating entanglement between the system of interest and a series of ancillary two-level systems, as depicted in Fig. 1(a). Measuring the ancillas generates so-called quantum trajectories [cf. Fig. 1(b)] which carry information on the dynamical evolution of the system. We show how to bias the properties of these trajectories, such as the rate of certain measurement outcomes on the ancillas and their temporal correlations. Our biasing protocol relies on interpreting a trajectory as a microstate of a fictitious spin system. Defining an "energy" function similar to that of the Ising model, we derive a dynamics, which enhances or reduces the probability of

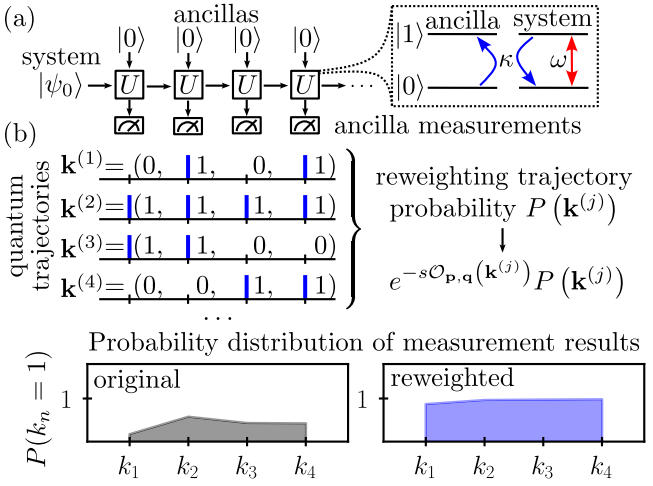

FIG. 1. Open-system dynamics and quantum trajectories in the collision model. (a) The two-level system, in the initial state $|\psi_0\rangle$, collides sequentially with ancillas (also two-level systems) all prepared in the $|0\rangle$ state. During a collision the system and an ancilla interact via an exchange interaction visualized in the inset; see also Eq. (1). (b) The outcomes k_n of projective measurements on the ancillas produce a quantum trajectory, whose jth realization is denoted by $\mathbf{k}^{(j)}=(k_1^{(j)},\ldots,k_N^{(j)})$. This trajectory occurs with a probability $P(\mathbf{k}^{(j)})$. We formally bias the statistics of the ensemble of trajectories by reweighting the probabilities with respect to the "energy" function $\mathcal{O}_{\mathbf{p},\mathbf{q}}(\mathbf{k})$, where $\mathbf{p}$ and $\mathbf{q}$ are coupling constants and s can be interpreted as "inverse temperature." The probability distribution for observing the outcome $k_n=1$, when measuring the state of the nth ancilla, is shown at the bottom, for the original as well as the reweighted, i.e., biased, ensemble.

certain trajectories in close resemblance to the Boltzmann weight of equilibrium statistical mechanics, as highlighted in Fig. 1(b). We show how such a deformed—at first glance unphysical—probability can be obtained on a quantum computer. Our study broadens the spectrum of use cases for quantum computers within the domain of nonequilibrium quantum systems, and provides first proof-of-principle results on the `ibmq_jakarta` machine.

Collision model.—We consider a quantum system subject to a Markovian discrete-time collision-model dynamics, illustrated in Fig. 1(a). The system state is encoded in the pure state $|\psi\rangle$ and, within each discrete time step, it collides with an ancillary two-level system described through the computational basis $\{|0\rangle, |1\rangle\}$. We assume that each ancilla is initialized in the reference state $|0\rangle$ and that the system-ancilla interaction is described by a unitary $U = e^{-ih}$, with h a Hermitian operator. After the collision, the ancilla is measured in the computational basis. This results in a stochastic evolution for the system described in terms of Kraus operators $K_k = \langle k|U|0\rangle$ [30,31]. Indeed, with probability $P_k = \|K_k|\psi\rangle\|^2$, the measurement outcome k is observed for the ancilla and the system evolves as $[(K_k|\psi\rangle)/\sqrt{P_k}]$. Performing N collisions and measurements yields a quantum trajectory $\mathbf{k} = (k_1, \ldots, k_N)$ as shown in Fig. 1(b). The probability for the occurrence of a specific trajectory is $P(\mathbf{k}) = \|K_{k_N} \ldots K_{k_1}|\psi_0\rangle\|^2$. The discrete-time dynamics of the state of the system, averaged over all possible measurement outcomes, is described by the Kraus map $\mathcal{E}[\rho] = \sum_k K_k \rho K_k^\dagger$.

We study here the simplest case in which the system is a two-level system, just like the ancillas. Furthermore, we set

$$h = \omega(\mathbb{1} \otimes \sigma_x) + \kappa(\sigma_+ \otimes \sigma_- + \sigma_- \otimes \sigma_+), \tag{1}$$

with $\sigma_- = \sigma_+^\dagger = |0\rangle\langle 1|$ and $\sigma_x = \sigma_- + \sigma_+$. Throughout, we set the parameters to $\omega = \kappa = 1$ and select $|\psi_0\rangle = |0\rangle$ as the initial state of the system. Contrarily to this genuine discrete-time dynamics, by introducing a time unit Δt together with the rescaling $\omega \to \omega\Delta t$ and $\kappa \to \sqrt{\kappa\Delta t}$, we note that the system dynamics converges in the limit $\Delta t \to 0$ toward the continuous-time Lindblad equation of a two-level atom with Rabi frequency ω and decay rate κ (see the Supplemental Material [34] for details).

Biased quantum trajectories.—Given that the ancillas are two-level systems, each quantum trajectory $\mathbf{k} = (k_1, \ldots, k_N)$ is a sequence of zeros and ones. Within a thermodynamic analogy (see also, e.g., Refs. [38–42]), each of these sequences can be interpreted as a microscopic configuration (microstate) of a fictitious one-dimensional Ising spin system. The probability over these microstates is then given by $P(\mathbf{k})$. In the standard thermodynamic approach, $P(\mathbf{k})$ is assumed to be a flat probability [39]. Here, however, the collision model provides, in general, a nonflat probability $P(\mathbf{k})$, which nevertheless does not spoil the thermodynamic analogy. Our goal is to reweigh (or bias) this probability by using an "energy" function [see Fig. 1(b)]

$$\mathcal{O}_{\mathbf{p},\mathbf{q}}(\mathbf{k}) = \sum_{n=1}^{N} p_n k_n + \sum_{\substack{n,m=1 \\ n>m}}^{N} q_{nm} k_n k_m, \tag{2}$$

defined in terms of the set of real coefficients $\{p_n, q_{nm}\}$. In analogy with the Ising model, the vector $\mathbf{p} = (p_1, \ldots, p_N)$ encodes the interaction of the spin system with an (possibly inhomogeneous) external field, while the matrix $\mathbf{q}$, collecting all the terms q_{nm}, describes the two-spin interacting energy. The reweighting (or biasing) is formally achieved by introducing the *canonical* Gibbs probability $P(\mathbf{k}, s) \propto e^{-s\mathcal{O}_{\mathbf{p},\mathbf{q}}(\mathbf{k})} P(\mathbf{k})$, in which $e^{-s\mathcal{O}_{\mathbf{p},\mathbf{q}}(\mathbf{k})}$ represents a Boltzmann weight. Within this thermodynamic construction, the parameter s in the biasing factor serves as an "inverse temperature" [35,40,43]. The probability of the different quantum trajectories is then modified on demand by tuning the "temperature," as well as the "energy" function, such that the outcome of the measurements tends to minimize $s\mathcal{O}_{\mathbf{p},\mathbf{q}}(\mathbf{k})$. This allows one to steer the properties of the quantum trajectories, such as the frequency of certain measurement outcomes and interestingly also their correlations. As we demonstrate below, it is possible to devise an appropriate system-ancilla interaction such that the so-far artificially constructed reweighted ensemble $P(\mathbf{k}, s)$ becomes the physical ensemble of a bona-fide collision-model dynamics, which can be implemented on a quantum computer.

Noninteracting "energy" function.—We first consider a simple "energy" function, which solely contains external fields, $\mathbf{p} = (p_1, \ldots, p_N)$, i.e.,

$$\mathcal{O}_{\mathbf{p}}(\mathbf{k}) = \sum_{n=1}^{N} p_n k_n = \mathbf{p} \cdot \mathbf{k}. \tag{3}$$

To generate the reweighted ensemble $P(\mathbf{k}, s)$ we exploit an auxiliary quantum map, the so-called tilted Kraus map, which biases the probability of each quantum trajectory through the desired factor $e^{-s\mathcal{O}_{\mathbf{p}}(\mathbf{k})}$. This tilted map reads, for a single time step, as

$$\mathcal{E}_{s_n}[\rho] = K_0 \rho K_0^\dagger + e^{-s_n} K_1 \rho K_1^\dagger,$$

with $s_n = s p_n$. While assigning the correct weights to the different trajectories, this map does not implement a physical dynamics since, for $s_n \neq 0$, it violates trace preservation [31,35,36]. Nonetheless, a physical process described by the reweighted ensemble [44] can be constructed [34]. It consists of a map with, in general, time-dependent (i.e. dependent on the collision number n) Kraus operators

$$\tilde{K}_0^n = G_n K_0 G_{n-1}^{-1}, \tag{4}$$

$$\tilde{K}_1^n = e^{-s_n/2} G_n K_1 G_{n-1}^{-1} \tag{5}$$

for the nth collision. Moreover, the initial state needs to be rotated according to

$$R_i|\psi_0\rangle = \frac{G_0|\psi_0\rangle}{\|G_0|\psi_0\rangle\|}. \tag{6}$$

The Hermitian matrices G_n, are given recursively as

$$G_{n-1} = \sqrt{\mathcal{E}_{s_n}^*[G_n^2]}, \tag{7}$$

using the dual tilted Kraus map $\mathcal{E}_{s_n}^*$ and setting the final-time condition $G_N = \mathbb{1}$ (see the Supplemental Material [34] for details).

In the following we discuss a few examples, for which the corresponding data are shown in Fig. 2. The simplest case [panel (a)] is that of a uniform field, $p_n = 1$. According to the sign of s, this choice increases or decreases the probability of quantum trajectories according to the total amount of $k_n = 1$ measurement outcomes they contain [see also Fig. 1(b)]. Conversely, with a staggered field [panel (b)] $p_n = (-1)^n$ we can bias quantum trajectories toward an imbalance between odd and even spins, i.e., showing alternating measurement outcomes at odd and even times. An even more general case [panel (c)] is that of a random sequence of local external fields, i.e., $p_n \in \{\pm 1\}$. In Fig. 2 we show numerical results obtained for all three cases. The black data show the probabilities of the original, i.e., unbiased, dynamics. Throughout, we observe that for a positive value of s (red data) the probability of trajectories that minimize the scalar product $\mathbf{p}\cdot\mathbf{k}$, i.e., the "energy" function (3), is enhanced. Conversely, for negative s trajectories that maximize $\mathbf{p}\cdot\mathbf{k}$ become dominant.

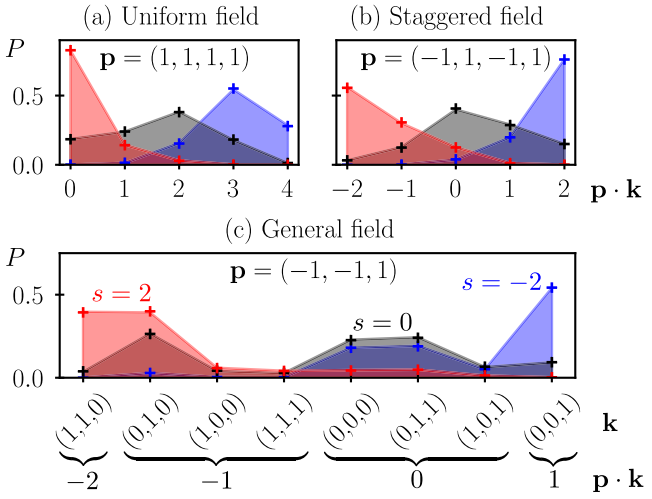

FIG. 2. Noninteracting "energy" function. (a),(b) Shown is the probability P for obtaining a trajectory with a given value of $\mathbf{p}\cdot\mathbf{k}$. The black data correspond to the original, i.e., unbiased, process ($s = 0$), while the red (blue) data correspond to the biased process with $s = 2$ ($s = -2$). Each dataset contains two subsets: the lines above the shaded areas are numerically exact results, obtained from computing the probabilities $P(\mathbf{k}) = \|K_{k_N}\ldots K_{k_1}|\psi_0\rangle\|^2$ and reweighting them appropriately. The crosses are obtained by classically simulating 20 000 trajectories generated from the biased Kraus map, Eqs. (4) and (5). The statistical error is smaller than the marker size. In panel (c) we show the probability as a function of $\mathbf{p}\cdot\mathbf{k}$ and also at the level of individual trajectories $\mathbf{k}$.

In the following we show how the biased dynamics can be implemented on an actual digital quantum processor. To do this, we first need to unravel the Kraus map defined by the operators $\{\tilde{K}_{k_n}^n\}_{k_n=0}^1$ into a unitary collision model with an auxiliary ancilla [17]. The existence of such a unitary is guaranteed by the Stinespring dilation theorem [11,45]. The desired Kraus operators are obtained when choosing for the nth collision the operator (see the Supplemental Material [34] for details)

$$\tilde{U}_n = \left(\begin{array}{c|c} \tilde{K}_0^n & \cdots \\ \tilde{K}_1^n & \cdots \end{array}\right). \tag{8}$$

The rectangular submatrix containing $\tilde{K}_0^n$ and $\tilde{K}_1^n$ is an isometry, since $\tilde{K}_0^{n\dagger}\tilde{K}_0^n + \tilde{K}_1^{n\dagger}\tilde{K}_1^n = \mathbb{1}$. The other columns do not participate to the collision-model dynamics, and we can thus fill them with additional orthogonal column vectors. In this way, the isometry is promoted to a unitary operator encoding the system-ancilla collision. This

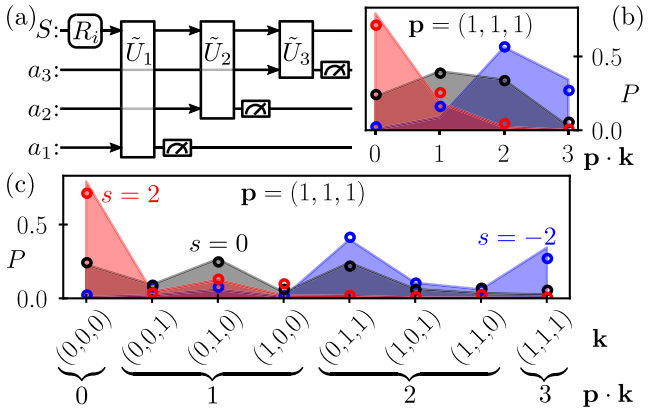

FIG. 3. Quantum simulations of the biased dynamics for a uniform field. (a) The quantum circuit used to implement the biased dynamics consists of an initial rotation R_i applied to the system S as well as adapted collision unitaries $\tilde{U}_n$. Arrows indicate which qubits collide. The transpiled version of this quantum circuit is run on the `ibmq_jakarta` quantum processor. The obtained data are evaluated with respect to (b) the "energy" $\mathbf{p}\cdot\mathbf{k}$ and (c) the individual trajectories $\mathbf{k}$. We used 20 000 samples.

procedure allows us to construct the quantum circuit shown in Fig. 3(a), which must be transpiled using the gates available for the chosen quantum processor, a task which is left unsupervised to the Qiskit library [37].

In Figs. 3(b) and 3(c), we show results from quantum simulations of our trajectories on the 7-qubit quantum processor `ibmq_jakarta`. The obtained probabilities for the original and the modified trajectory ensemble (circles) show good agreement with the exact probabilities (shaded), both as a function of the scalar product $\mathbf{p}\cdot\mathbf{k}$ and at the level of individual trajectories $\mathbf{k}$. In contrast to the classical simulation results, displayed in Fig. 2, some deviations can be observed, that exceed the statistical error bounds (which are smaller than the marker size). This points toward the presence of a systematic error in the quantum processor due to a noisy implementation of the unitary gates [5–7,46–48].

Interacting "energy" function.—We now turn to the more interesting case of interacting "energy" functions, which permit the bias of time correlations among ancillary measurements within quantum trajectories. For concreteness, we consider here the following nearest-neighbor function

$$\mathcal{O}_{\mathrm{NN}}(\mathbf{k}) = \sum_{n=2}^{N} \sigma_n \sigma_{n-1}, \tag{9}$$

with $\sigma_n = 1-2k_n$. In our thermodynamic analogy, this function corresponds to a classical Ising energy, and large values of $\mathcal{O}_{\mathrm{NN}}(\mathbf{k})$ are associated with microstates in which neighboring spins are aligned, i.e., measurements on consecutive ancillas yield the same outcome. Compared with noninteracting "energy" functions, this case is more challenging to treat since the biasing at a given discrete-time step n depends on the outcome of the measurement of the previous ancilla's state. The ensuing tilted map needs to involve all collisions and can no longer be split into independent maps. It reads (see the Supplemental Material [34] for details) as

$$\rho \to \sum_{\mathbf{k}\in\{0,1\}^N} (T_s)_{k_N,k_{N-1}} \circ \ldots \circ (T_s)_{k_2,k_1} \circ (T_s)_{k_1}[\rho],$$

where

$$(T_s)_{k_n,k_{n-1}}[\rho] = e^{-s\sigma_n\sigma_{n-1}} K_{k_n} \rho K_{k_n}^{\dagger} \tag{10}$$

and $(T_s)_{k_1}[\rho] = K_{k_1}\rho K_{k_1}^{\dagger}$. The matrices T_s are transfer matrices with entries given by maps rather than numbers. As for the noninteracting case, the tilted map cannot describe a physical process since it is not trace preserving for $s \neq 0$. Nonetheless, an actual physical process that creates the reweighted ensemble can be found also in this case of interacting "energy" functions. For the nth collision this is defined by the Kraus operators $\{\tilde{K}^n_{k_n|k_{n-1}}\}_{k_n=0}^{1}$ *conditioned* on the outcome k_{n-1} of the measurement at time $n-1$ and given by

$$\tilde{K}^n_{k_n|k_{n-1}} = e^{-s\sigma_n\sigma_{n-1}/2} G_{n|k_n} K_{k_n} G^{-1}_{n-1|k_{n-1}}, \tag{11}$$

with

$$G_{n-1|k_{n-1}} = \sqrt{\sum_{k_n=0}^{1} (T_s^*)_{k_n,k_{n-1}}[G^2_{n|k_n}]}, \tag{12}$$

setting $G_{N|k_N} = \mathbb{1}$ for all k_N. We note, that $G_{0|0} = G_{0|1} = G_0$ and the initial state is modified according to the rotation given by Eq. (6). This construction can be extended to more general "energy" functions, for example functions which depend on strings of measurement outcomes, $k_1k_2k_3\ldots k_N$. This allows one to modify any n-time correlation function of the trajectory ensemble.

To implement this conditioned non-Markovian biased dynamics on a quantum processor, the first step is once again to promote each conditioned Kraus map, given by the operators in Eq. (11), into a unitary collision, $\tilde{U}_{n|k_{n-1}}$, with an ancilla, in analogy to Eq. (8). Then, we introduce the projector on the state of the ancilla $|k_{n-1}\rangle\langle k_{n-1}|$ at time step $n-1$ and construct the 3-qubit unitary

$$\tilde{V}_n = \sum_{k_{n-1}} |k_{n-1}\rangle\langle k_{n-1}| \otimes \tilde{U}_{n|k_{n-1}},$$

which implements the collision $\tilde{U}_{n|k_{n-1}}$ on the system and on the nth ancilla, according to the outcome of the measurement k_{n-1} on the previous ancilla. The structure of these unitaries further highlights the non-Markovian character of the biased dynamics, which thus takes the form of an *extended collision model*. The corresponding quantum circuit is shown in Fig. 4(a).

In Figs. 4(b) and 4(c) we report results from both classical numerical simulation (crosses) and the quantum simulations (circles) of this biased dynamics. As anticipated, the classical simulation results, obtained from trajectory sampling, agree excellently with the reweighted probabilities. However, the probabilities sampled via the quantum simulations display significant systematic errors, both when plotted as a function of $\mathcal{O}_{\mathrm{NN}}$ and when resolved for individual trajectories $\mathbf{k}$. We attribute these errors to the substantial depth of the transpiled circuit, which is mainly due to the representation of the 3-qubit gates in terms of the basis gates of the device [17]: even small single-gate errors, as for instance the controlled NOT error which is smaller than 1% according to the most recent calibration, accumulate and give rise to an effective dynamics which is rather different from the desired one [19]. To our understanding, simple error mitigation techniques regarding measurement errors [20] or zero-noise extrapolation [10] are not sufficient to eliminate the noise introduced in the dynamics, at least not when using the unsupervised transpiling of the circuit. In the Supplemental Material [34] we

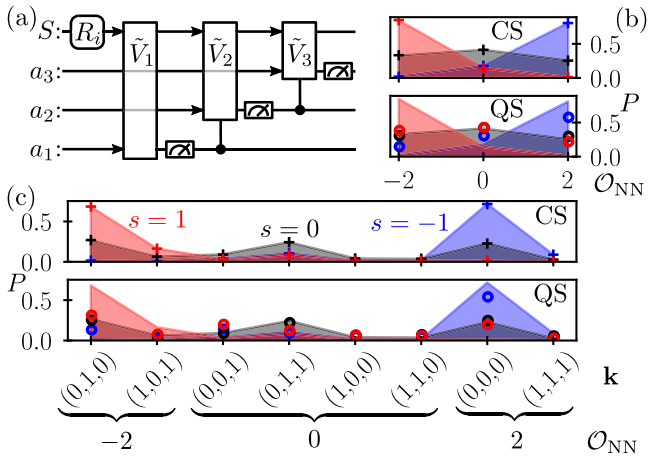

FIG. 4. Biasing correlations within quantum trajectories. (a) Quantum circuit for the biased dynamics with the interacting "energy" function $\mathcal{O}_{\mathrm{NN}}$ in Eq. (9). Here, R_i represents the required rotation of the initial state and the $\tilde{V}_{n>1}$ are conditioned unitaries (see main text). (b),(c) Probability for obtaining trajectories with given $\mathcal{O}_{\mathrm{NN}}$ and $\mathbf{k}$, respectively. The black data correspond to the original, i.e., unbiased, process ($s = 0$), while the red (blue) data correspond to the biased process with $s = 1$ ($s = -1$). Each dataset contains two subsets: the lines above the shaded areas are numerically exact results, obtained from the (tilted) dynamical map. Top panels (CS) are obtained by classically simulating 20 000 trajectories of the biased dynamics. Bottom panels (QS) are obtained by sampling the same number of trajectories on the quantum processor `ibmq_jakarta`.

discuss how Qiskit allows for an *a priori* estimate on the errors to be expected from the quantum simulations.

Conclusions.—We have shown how to bias the dynamical behavior, e.g., the temporal correlations, of the output of open quantum systems on a quantum computer. Our approach is based on a thermodynamic analogy, where the probability of a given trajectory is modified through an "energy" function. Simple, i.e., noninteracting, "energy" functions can be rather reliably implemented. However, the inclusion of interactions in order to enhance correlations between output measurements on the ancillas appears to exhaust the capability of the `ibmq_jakarta` machine, on which we conducted our study. The ultimate reason appears to be that the interacting case requires the implementation of three-body gates, which are transpiled into relatively deep circuits. This shows that already the quantum simulation and manipulation of short trajectories of a two-level system is a difficult task and illustrates the enormous challenge of faithfully simulating and engineering open many-body quantum dynamics with quantum computers. Advances in circuit design, such as dynamic circuits that allow *in situ* feedback based on measurement results, may help to improve this situation [49,50]. Also, the ability of resetting and reusing ancillas will of course allow one to implement more collisions and thus longer evolution times. So far, we calculated the quantum circuit yielding the biased dynamics in advance on a classical computer. In the future it would be interesting to investigate whether this is indeed necessary or whether the corresponding maps can be directly computed and implemented on a quantum device.

The code and the data that support the findings of this Letter are available on Zenodo [51].

We thank Markus Müller, Juan P. Garrahan, and Hugo Touchette for fruitful discussions. We acknowledge funding from the Deutsche Forschungsgemeinschaft (DFG, German Research Foundation) under Project No. 435696605 and through the Research Unit FOR 5413/1, Grant No. 465199066, and through the Research Unit FOR 5522/1, Grant No. 499180199. This project has also received funding from the European Union's Horizon Europe research and innovation program under Grant Agreement No. 101046968 (BRISQ). F. C. is indebted to the Baden-Württemberg Stiftung for the financial support of this research project by the Eliteprogramme for Postdocs.

[1] D. P. DiVincenzo, The physical implementation of quantum computation, Fortschr. Phys. **48**, 771 (2000).
[2] J. Preskill, Quantum computing 40 years later, arXiv:2106.10522.
[3] R. Blume-Kohout, C. M. Caves, and I. H. Deutsch, Climbing mount scalable: Physical resource requirements for a scalable quantum computer, Found. Phys. **32**, 1641 (2002).
[4] M. A. Nielsen and I. L. Chuang, *Quantum Computation and Quantum Information: 10th Anniversary Edition* (Cambridge University Press, Cambridge, England, 2010).
[5] J. Preskill, Quantum Computing in the NISQ era and beyond, Quantum **2**, 79 (2018).
[6] J. W. Z. Lau, K. H. Lim, H. Shrotriya, and L. C. Kwek, NISQ computing: Where are we and where do we go?, AAPPS Bull. **32**, 27 (2022).
[7] F. Leymann and J. Barzen, The bitter truth about gate-based quantum algorithms in the NISQ era, Quantum Sci. Technol. **5**, 044007 (2020).
[8] R. P. Feynman, Simulating physics with computers, Int. J. Theor. Phys. **21**, 467 (1982).
[9] F. Arute, K. Arya, R. Babbush, D. Bacon, J. C. Bardin *et al.*, Quantum supremacy using a programmable superconducting processor, Nature (London) **574**, 505 (2019).
[10] N. Keenan, N. Robertson, T. Murphy, S. Zhuk, and J. Goold, Evidence of Kardar-Parisi-Zhang scaling on a digital quantum simulator, npj Quantum Inf. **9**, 72 (2023).
[11] A. J. Friedman, O. Hart, and R. Nandkishore, Measurement-induced phases of matter require adaptive dynamics, arXiv:2210.07256.
[12] A. J. Daley, I. Bloch, C. Kokail, S. Flannigan, N. Pearson, M. Troyer, and P. Zoller, Practical quantum advantage in quantum simulation, Nature (London) **607**, 667 (2022).
[13] Y. Kim, C. J. Wood, T. J. Yoder, S. T. Merkel, J. M. Gambetta, K. Temme, and A. Kandala, Scalable error mitigation for noisy quantum circuits produces competitive expectation values, Nat. Phys. **19**, 752 (2023).

[14] A. D. Córcoles, M. Takita, K. Inoue, S. Lekuch, Z. K. Minev, J. M. Chow, and J. M. Gambetta, Exploiting Dynamic Quantum Circuits in a Quantum Algorithm with Superconducting Qubits, Phys. Rev. Lett. **127**, 100501 (2021).

[15] I. Buluta and F. Nori, Quantum simulators, Science **326**, 108 (2009).

[16] A. Francis, D. Zhu, C. H. Alderete, S. Johri, X. Xiao, J. K. Freericks, C. Monroe, N. M. Linke, and A. F. Kemper, Many-body thermodynamics on quantum computers via partition function zeros, Sci. Adv. **7**, eabf2447 (2021).

[17] S. Leontica, F. Tennie, and T. Farrow, Simulating molecules on a cloud-based 5-qubit IBM-Q universal quantum computer, Commun. Phys. **4**, 112 (2021).

[18] X. Xiao, J. K. Freericks, and A. F. Kemper, Determining quantum phase diagrams of topological Kitaev-inspired models on NISQ quantum hardware, Quantum **5**, 553 (2021).

[19] A. Smith, M. S. Kim, F. Pollmann, and J. Knolle, Simulating quantum many-body dynamics on a current digital quantum computer, npj Quantum Inf. **5**, 106 (2019).

[20] G. García-Pérez, M. A. C. Rossi, and S. Maniscalco, IBM Q experience as a versatile experimental testbed for simulating open quantum systems, npj Quantum Inf. **6**, 1 (2020).

[21] D. A. Chisholm, G. García-Pérez, M. A. C. Rossi, S. Maniscalco, and G. M. Palma, Witnessing objectivity on a quantum computer, Quantum Sci. Technol. **7**, 015022 (2021).

[22] M. Cattaneo, M. A. C. Rossi, G. García-Pérez, R. Zambrini, and S. Maniscalco, Quantum simulation of dissipative collective effects on noisy quantum computers, PRX Quantum **4**, 010324 (2023).

[23] J. T. Barreiro, M. Müller, P. Schindler, D. Nigg, T. Monz, Michael Chwalla, M. Hennrich, C. F. Roos, P. Zoller, and R. Blatt, An open-system quantum simulator with trapped ions, Nature (London) **470**, 486 (2011).

[24] P. Schindler, M. Müller, D. Nigg, J. T. Barreiro, E. A. Martinez, M. Hennrich, T. Monz, S. Diehl, P. Zoller, and R. Blatt, Quantum simulation of dynamical maps with trapped ions, Nat. Phys. **9**, 361 (2013).

[25] H. Lu, C. Liu, D.-S. Wang, L.-K. Chen, Z.-D. Li *et al.*, Experimental quantum channel simulation, Phys. Rev. A **95**, 042310 (2017).

[26] T. Xin, S.-J. Wei, J. S. Pedernales, E. Solano, and G.-L. Long, Quantum simulation of quantum channels in nuclear magnetic resonance, Phys. Rev. A **96**, 062303 (2017).

[27] Z. Hu, R. Xia, and S. Kais, A quantum algorithm for evolving open quantum dynamics on quantum computing devices, Sci. Rep. **10**, 3301 (2020).

[28] H. Kamakari, S.-N. Sun, M. Motta, and A. J. Minnich, Digital quantum simulation of open quantum systems using quantum imaginary–time evolution, PRX Quantum **3**, 010320 (2022).

[29] X. Mi, A. A. Michailidis, S. Shabani, K. C. Miao, P. V. Klimov *et al.*, Stable quantum-correlated many body states via engineered dissipation, arXiv:2304.13878.

[30] F. Ciccarello, S. Lorenzo, V. Giovannetti, and G. M. Palma, Quantum collision models: Open system dynamics from repeated interactions, Phys. Rep. **954**, 1 (2022).

[31] D. Cilluffo, G. Buonaiuto, I. Lesanovsky, A. Carollo, S. Lorenzo, G. Massimo Palma, F. Ciccarello, and F. Carollo, Microscopic biasing of discrete-time quantum trajectories, Quantum Sci. Technol. **6**, 045011 (2021).

[32] M. van Horssen and M. Guţă, Sanov and central limit theorems for output statistics of quantum Markov chains, J. Math. Phys. (N.Y.) **56**, 022109 (2015).

[33] M. Ziman, P. Štelmachovič, and V. Bužk, Description of quantum dynamics of open systems based on collision-like models, Open Syst. Inf. Dyn. **12**, 81 (2005).

[34] See Supplemental Material at http://link.aps.org/supplemental/10.1103/PhysRevLett.131.120401, which further contains Refs. [35–37], for details.

[35] J. P. Garrahan and I. Lesanovsky, Thermodynamics of Quantum Jump Trajectories, Phys. Rev. Lett. **104**, 160601 (2010).

[36] F. Carollo, J. P. Garrahan, I. Lesanovsky, and C. Pérez-Espigares, Making rare events typical in Markovian open quantum systems, Phys. Rev. A **98**, 010103(R) (2018).

[37] Qiskit contributors, Qiskit: An open-source framework for quantum computing (2023), 10.5281/zenodo.2573505.

[38] V. Lecomte, C. Appert-Rolland, and F. van Wijland, Thermodynamic formalism for systems with Markov dynamics, J. Stat. Phys. **127**, 51 (2007).

[39] H. Touchette, The large deviation approach to statistical mechanics, Phys. Rep. **478**, 1 (2009).

[40] J. P. Garrahan, R. L. Jack, V. Lecomte, E. Pitard, K. van Duijvendijk, and F. van Wijland, First-order dynamical phase transition in models of glasses: An approach based on ensembles of histories, J. Phys. A **42**, 075007 (2009).

[41] R. Chetrite and H. Touchette, Nonequilibrium Microcanonical and Canonical Ensembles and Their Equivalence, Phys. Rev. Lett. **111**, 120601 (2013).

[42] R. Chetrite and H. Touchette, Variational and optimal control representations of conditioned and driven processes, J. Stat. Mech. (2015) P12001.

[43] F. Carollo, R. L. Jack, and J. P. Garrahan, Unraveling the Large Deviation Statistics of Markovian Open Quantum Systems, Phys. Rev. Lett. **122**, 130605 (2019).

[44] R. L. Jack and P. Sollich, Large deviations and ensembles of trajectories in stochastic models, Prog. Theor. Phys. Suppl. **184**, 304 (2010).

[45] W. F. Stinespring, Positive functions on C*-algebras, Proc. Am. Math. Soc. **6**, 211 (1955).

[46] G. Di Bartolomeo, M. Vischi, F. Cesa, M. Grossi, S. Donadi, and A. Bassi, A novel approach to noisy gates for simulating quantum computers, arXiv:2301.04173.

[47] J. Liu and H. Zhou, Reliability modeling of NISQ-era quantum computers, in *2020 IEEE International Symposium on Workload Characterization (IISWC)* (IEEE, Beijing, China, 2020), pp. 94–105.

[48] M. L. Dahlhauser and T. S. Humble, Modeling noisy quantum circuits using experimental characterization, Phys. Rev. A **103**, 042603 (2021).

[49] A. Cross, A. Javadi-Abhari, T. Alexander, N. De Beaudrap, L. S. Bishop *et al.*, OpenQASM 3: A broader and deeper quantum assembly language, ACM Trans. Quantum Comput. **3**, 1 (2022).

[50] D. C. McKay, T. Alexander, L. Bello, M. J. Biercuk, L. Bishop *et al.*, Qiskit backend specifications for OpenQASM and OpenPulse experiments, arXiv:1809.03452.

[51] M. Cech, I. Lesanovsky, and F. Carollo, Data of "Thermodynamics of quantum trajectories on a quantum computer" (2023), 10.5281/zenodo.8060040.